

1 **Large-scale crustal structure beneath Singapore using**  
2 **receiver functions from a dense urban nodal array**

3 **Karen H. Lythgoe<sup>1</sup>, Miranda Ong Su Qing<sup>1</sup>, Shengji Wei<sup>1</sup>**

4 <sup>1</sup>Earth Observatory of Singapore, Nanyang Technological University, Singapore

5 **Key Points:**

- 6 • Robust receiver functions are generated from a temporary dense nodal array in  
7 a noisy urban environment.
- 8 • High frequency receiver functions reveal Singapore's crustal structure with direct  
9 implications for seismic hazard analysis.
- 10 • Azimuthal variations reveal distinct crustal structure on either side of the Bukit  
11 Timah fault.

---

Corresponding author: Karen Lythgoe, [karen.lythgoe@ntu.edu.sg](mailto:karen.lythgoe@ntu.edu.sg)

**Abstract**

Geophysics has a role to play in the development of 'smart cities', for example through geohazard mitigation and subsurface imaging for underground construction. This is particularly true for Singapore, one of the world's most densely populated countries. Imaging of Singapore's subsurface is required to identify geological faults, model shaking from future earthquakes and provide a framework for underground development. A non-invasive geophysical technique that is well suited for urban areas is passive seismic surveys using nodes. Here, we image Singapore's crustal structure using receiver functions generated by a 40-day deployment of a dense nodal array. We generate high resolution receiver functions, despite the noisy environment and short recording time and also create common-conversion point images. Our results reveal a complex crustal structure, containing multiple discontinuities. Azimuthal variations indicate a distinct change in crustal structure on either side of the postulated Bukit Timah fault, which has implications for seismic hazard.

**Plain Language Summary**

By 2050 over two thirds of the global population is expected to live in cities (United Nations, 2018). Rapid urbanisation creates an ever pressing need to understand the subsurface of our cities, for example for underground development. Such dense population centres also increase the exposure to nearby natural hazards such as earthquakes. One technological advancement that allows us to image the subsurface of cities are passive seismic surveys using nodes. Nodes are small seismic instruments that can be deployed in urban areas such as schools and parks. We present results of a passive seismic survey using 88 nodes deployed in Singapore for 40 days. We generate high resolution receiver functions across the array, despite the short recording time, by using array stacking techniques. The dense nature of the array also allows continuous high frequency signals to be traced. Our results reveal that the structure of the crust is very different on either side of the Bukit Timah fault, which agrees with geological information. Ancient faults in peninsula Malaysia have been reactivated in the recent past due to stress transfer from the Sumatran subduction zone, therefore this geological fault under a densely populated urban centre warrants further study for seismic hazard.

## 1 Introduction

Increasing urbanisation creates an ever pressing need to understand the subsurface of our cities. 'Smart' cities aim to use technology to improve their liveability, economic and environmental stability. Geophysics, and seismology in particular, has a role to play in smart city development, for example through geohazard mitigation and subsurface imaging for underground construction. Technological advancements are allowing us to image cities in ways not previously possible. In particular, passive seismic surveys using nodes are a non-invasive acquisition advancement that are uniquely suitable for urban environments. Here we demonstrate one application of seismic nodes in the world's 'smartest city'.

Singapore is a densely populated city nation, and better understanding of its seismic hazard and subsurface structure is prescient. Singapore experiences shaking from earthquakes in Sumatra, which is only a few hundred kilometres away (Pan & Sun, 1996). The Mentawai segment of the Sumatran megathrust is the closest to Singapore and is predicted to rupture as a large earthquake in the near future (Sieh et al., 2008). Simulations of future earthquake scenarios in Singapore are needed to ensure it is properly prepared. Imaging the crustal structure below Singapore is also required for underground construction, resource development and identification of geological faults. Local geological faults pose an as yet unassessed seismic hazard. Although Singapore lies on the relatively stable Sunda continental shelf, old faults zones nearby have been reactivated due to stress transfer from the Sumatran megathrust. Several earthquakes, up to  $M_{7.5}$ , have occurred within the Malay peninsula during the instrumental time period (ISC, 2019). For example a series of earthquakes up to  $M_{7.3.7}$  in 2007-2009, occurred on a previously unidentified fault 20 km from Kuala Lumpur (Shuib, 2009). It is therefore important to identify significant geological faults, especially in areas of high population density.

Conventional seismic surveys to image crustal structure are not well suited to urban environments. Such surveys typically use a network of large semi-permanent seismometers that use up valuable space and are deployed in relatively quiet environments. On the other hand, dense arrays of nodes are far better suited to urban environments. Seismic nodes can be deployed rapidly, directly into the ground and without any bulky equipment. Nodes – short period autonomous geophones - were originally developed in the energy industry for shallow land imaging with active sources (for example Manning

74 et al. (2019)). However several recent studies have demonstrated the utility of nodes for  
75 passive seismic imaging on a lithospheric scale (Ward et al., 2018; Liu et al., 2018; Wang  
76 et al., 2019; Lin et al., 2013). One drawback of nodes compared to conventional instru-  
77 ments is their short battery life of approximately 1 month. However, the considerable  
78 cost saving of nodes compared to conventional instruments permits the acquisition of very  
79 dense surveys and receiver density is the principle factor controlling subsurface image  
80 quality.

81 A key passive seismic technique to image crustal structure is the receiver function  
82 method (Langston, 1979; Vinnik, 1977). The technique employs body waves generated  
83 by teleseismic earthquakes to isolate mode conversions at discontinuities below a receiver.  
84 In order to increase the signal above the noise, receiver function imaging typically re-  
85 quires stacking of more than one year of teleseismic body waves at a single station (for  
86 example Macpherson et al. (2013)). The long-time needed normally limits the applica-  
87 tion of the technique to seismic stations that have been active for several years. How-  
88 ever nodal arrays can generate high resolution receiver functions despite their short record-  
89 ing time (Ward et al., 2018). This is because the dense station distribution permits stack-  
90 ing in space, in addition to stacking receiver functions over time. The close proximity  
91 of stations also permits higher frequency receiver functions to be used, since coherent  
92 mode conversions can be continuously traces between stations.

93 In this study, we image Singapore’s lithospheric structure using teleseismic receiver  
94 functions generated from a short-period nodal array. The motivation behind the nodal  
95 array was to 1) illuminate the large scale crustal structure beneath Singapore to provide  
96 a skeleton framework for future smart city refinement and 2) assess the performance of  
97 a nodal array in a noisy urban environment. We show that nodes are fully capable of  
98 generating high frequency receiver functions, even in a noisy environment with only 1  
99 month of data. Our results reveal a complex crustal structure, reflecting Singapore’s com-  
100 plicated geological history. Azimuthal variations in receiver functions indicate a distinct  
101 change in crustal structure on either side of the postulated Bukit Timah fault, which has  
102 implications for seismic hazard in the world’s third most densely populated country.

## 2 Geology of Singapore

The near surface geology of Singapore is relatively well known due to an abundance of shallow boreholes and building works. However the geological structure beyond several hundreds of meters is almost entirely unknown. The near surface is composed of three principle geological units – Bukit Timah granite, Jurong Group metasediment and quaternary sediments (Dodd et al., 2019) (Figure 1a). The Bukit Timah granite underlies central Singapore and is the most extensive geological unit. Quaternary sediments outcrop in eastern Singapore plus a small area in northern Singapore and overly Bukit Timah granite (Woon & Yingxin, 2009). The west of Singapore is composed of the Jurong Group – a sequence of lightly metamorphosed sediment that is highly folded and faulted (Leslie et al., 2019). The nature of the boundary between the Jurong Group and the Bukit Timah granite is not clear as the contact does not outcrop. One possibility is that the contact is an unconformity and that the Jurong Group also overlies Bukit Timah granite. Alternatively, the two units may be separated by a fault, often referred to as the Bukit Timah fault. The last geological unit is unconsolidated reclaimed land, which makes up over 20% of present-day Singapore.

## 3 Nodal array

A nodal array comprising 88 5Hz 3 component geophones was deployed across Singapore for a continuous 40-day period, from February to April 2019 (Figure 1a). Site locations were distributed across Singapore, with a denser profile located across the boundary between Bukit Timah granite and the Jurong Group. The largest station spacing was 8 km, for a node deployed on a nearby island. The smallest station spacing was 100 m for nodes deployed across the geological boundary. Site locations included parks, schools, nature reserves, weather stations, roadsides and industrial sites, and so had a range of ambient noise levels. In addition to the nodal array, 4 permanent seismic station operated by Singapore’s Meteorological Service, were used.

## 4 Methodology

Receiver functions are time series composed of P-to-S converted waves generated at structural boundaries in the Earth beneath a seismometer. Teleseismic P-waves are used to compute receiver functions as they approximate a vertically incident plane wave. We construct receiver functions for earthquakes larger than  $M_w 5.5$  with an epicentral

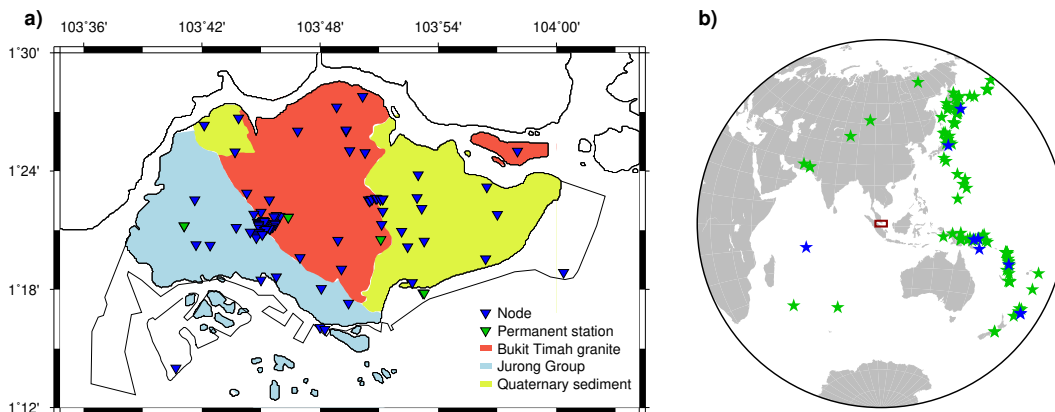


**Figure 1.** a) Map of Singapore showing broad geological units. Outer coastline marks the current coastline of Singapore which is built on reclaimed land. Blue triangles are locations of temporary nodes and green triangles are locations of permanent seismic stations. b) Earthquakes used to generate receiver functions. Blue stars show earthquakes used with the nodal array survey and green stars are earthquake used with the permanent stations.

134 distance from  $30^\circ$  to  $90^\circ$  - a total of 22 earthquakes during the acquisition time (Figure 1b).  
 135 We process the raw waveforms by deconvolving the instrument response, removing the  
 136 mean and linear trend, bandpass filtering from 0.05 – 10 Hz, and rotating the horizon-  
 137 tal components into radial and tangential components. Removing the instrument response  
 138 has the effect of boosting low frequencies relative to higher frequencies (Supplementary  
 139 Figure 1).

140 Receiver functions are generated by a time-domain iterative deconvolution with a  
 141 Gaussian low pass filter (Ligorria & Ammon, 1999). The Gaussian low pass filter removes  
 142 high-frequency noise in the receiver function at the expense of resolution. A Gaussian  
 143 width of 5 was chosen, which corresponds to a cut-off frequency of approximately 2.5 Hz.  
 144 This value reduces noise while keeping as much high frequency signal as possible (Sup-  
 145 plementary Figure 2). Using a dense nodal array in the United States, Ward et al. (2018)  
 146 generated receiver functions for a Gaussian value up to 10 (approximately 4.8 Hz). How-  
 147 ever in our case, such high Gaussian values generate noisy receiver functions, because  
 148 there is abundant man-made noise above approximately 3 Hz (Supplementary Figure 1  
 149 and 2). However our receiver functions still have over one octave more signal compared  
 150 to conventional surveys (for example Macpherson et al. (2013). The dense acquisition

151 means that coherent mode conversions can be traced between stations, which allows more  
152 high frequency signal to be utilised, even in an urban environment.

153 Receiver functions are quality controlled automatically and subsequently by visual  
154 inspection. From the 22 earthquakes that were used to generate receiver functions for  
155 the node data, 9 earthquakes produced receiver functions of sufficiently high quality. The  
156 earthquakes used to compute receiver functions are distributed in three azimuth bins:  
157  $280^\circ$  for earthquakes near Fiji,  $240^\circ$  for earthquake near Japan and  $75^\circ$  for one earthquake  
158 that occurred in the Indian Ocean. Receiver functions were also generated for four per-  
159 manent stations in operation in Singapore, composed of 1 broadband and 3 short-period  
160 instruments. On average 50 high quality receiver functions were generated per station  
161 from 229 suitable earthquakes ( $M_w$  greater than 5.5 in years 2012, 2013 and 2018).

## 162 **5 Results**

163 A receiver function profile across Singapore is shown in Figure 2. Stations within  
164 7 km are projected on to the profile, which strikes across the geological units. Receiver  
165 functions with an azimuth between  $200^\circ$  to  $300^\circ$  are stacked at each station - this is ap-  
166 proximately 90% of all high quality receiver functions and variations within this azimuth  
167 range are small. Receiver functions are also stacked in space. We stack all stations within  
168 a radius of 4 km, with the centre station doubly weighted. A radius of 4 km is chosen  
169 in this case to best increase signal while not smoothing across geological variations.

170 A clear Ps phase is seen at 4 seconds, matching the previous receiver functions of Macpherson  
171 et al. (2013). Additionally, intra-crustal discontinuities are present. In eastern Singapore  
172 there is a clear positive arrival between the direct P and Ps phases, with negative arrivals  
173 preceding and following the peak. This peak arrives at later times towards the centre  
174 of Singapore and then disappears completely. Conversely, western Singapore appears rel-  
175 atively homogeneous, with a negative arrival before Ps, which increases in amplitude fur-  
176 ther to the west.

177 In order to place the discontinuities at the correct location in depth, we utilise a  
178 migration method known as common-conversion point (CCP) stacking (Kosarev et al.,  
179 1999; Zhu et al., 2006). The amplitude at each point along the receiver function is back-  
180 projected to the conversion point using a background velocity model. We use a 1D ve-  
181 locity model generated by joint inversion of receiver functions and surface waves at a broad-

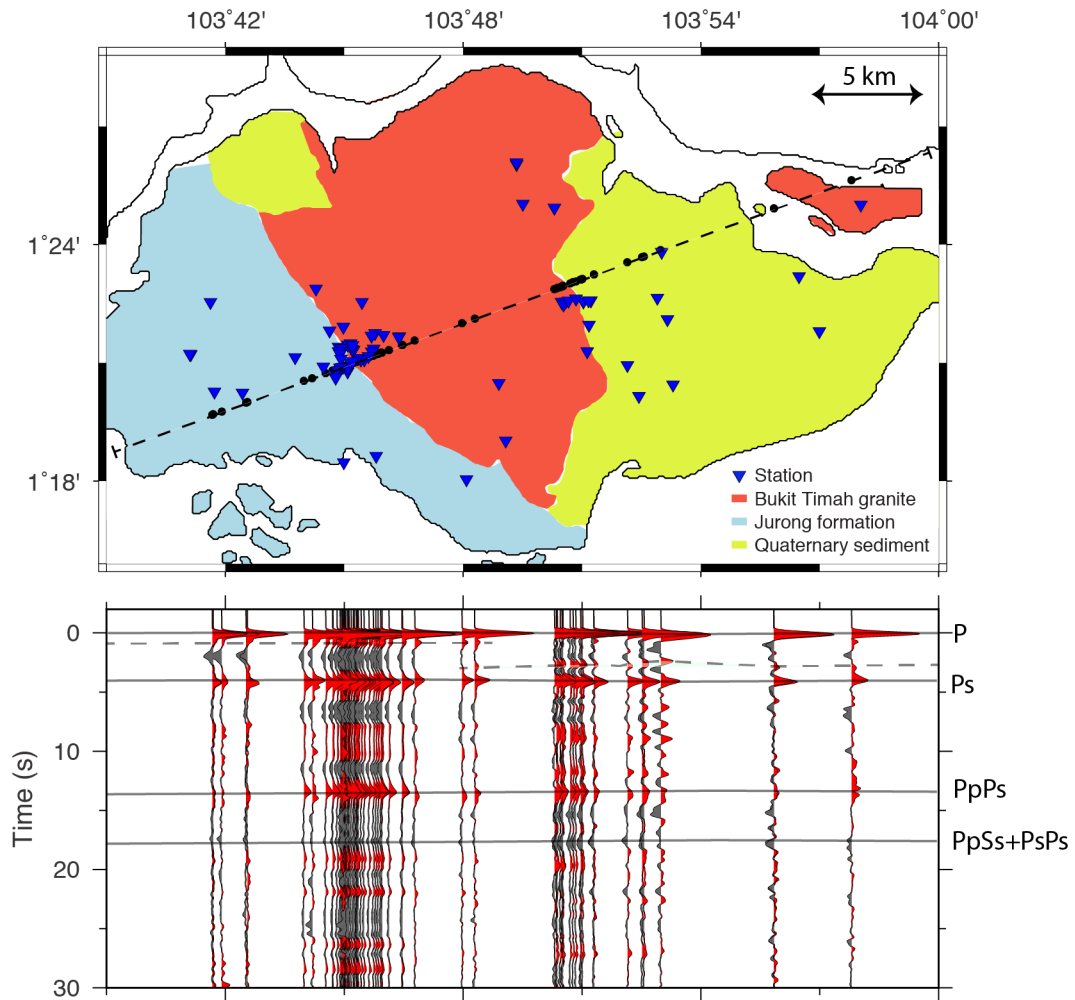


**Figure 2.** Receiver function profile across Singapore. Stations (blue triangles) within 7 km of the profile are projected on to the profile (black circles). Phase labels are based on predictions from a 30 km thick crust with an average P-wave velocity of 6 km/s and  $V_p/V_s$  of 1.78.

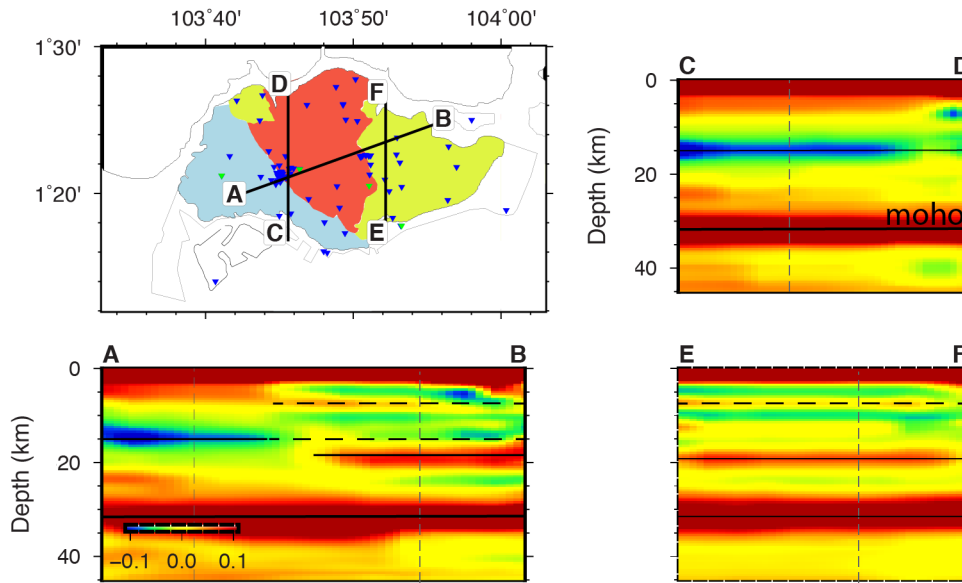


**Figure 3.** Common-conversion point images of the crust across Singapore.

182 band station in the centre of Singapore (Macpherson et al., 2013). After back-projection  
 183 of all receiver functions, the crustal volume is divided into bins and all amplitudes within  
 184 a bin are stacked, such that the amplitude of each bin represents the impedance contrast  
 185 at that location.

186 Figure 3 shows the resulting CCP image at several profiles. The moho is a high am-  
 187 plitude peak at 32 km depth. Macpherson et al. (2013) proposed that the depth to the  
 188 moho varied at a short wavelength across Singapore however we show that the moho depth  
 189 is constant. There are significant intra-crustal variations from west to east across Sin-  
 190 gapore. The negative arrival in western Singapore corresponds to the top of a low ve-  
 191 locity zone at 15 km depth. This trough appears to disappear towards the east, where  
 192 it is replaced by a peak at 19 km depth, marking the top of a high velocity layer. In the  
 193 east there is an additional low amplitude peak at 7 km depth. It is possible that this peak  
 194 continues to the west but it is not clearly separated from the main P arrival. The CCP  
 195 images show remarkably complex lateral variations over a distance of only 40 km.

196 The majority of teleseismic earthquakes occur to the east of Singapore and so imag-  
 197 ing is dominated by energy arriving from the east (azimuths of 240 - 280° from source  
 198 to receiver, Figure 1). Fortuitously, however, one suitable earthquake occurred in the In-  
 199 dian ocean during the nodal deployment and produced high quality receiver functions.

200 Seismic waves from the Indian ocean event travel to Singapore at an azimuth of  $75^\circ$ , il-  
201 luminating the far western side of Singapore (Figure 4). This is particularly useful for  
202 investigating variations in crustal structure from the Jurong Group to the Bukit Timah  
203 granite, across the postulated Bukit Timah fault.

204 Figure 4 shows receiver function profiles generated in the three azimuths groups.  
205 The piercepoints of rays at the base of the crust are shown in Figure 4a for each azimuth  
206 group. Waves arriving from an azimuth of  $75^\circ$  penetrate the crust of the Jurong Group,  
207 while the other azimuths sample the crust below the Bukit Timah granite. The receiver  
208 functions from an azimuth of  $75^\circ$  are dramatically different from the other azimuth groups.  
209 A peak at 2 seconds due to an intra-crustal boundary appears, with sharp negative ar-  
210 rivals surrounding the peak. On the other hand the profiles from azimuths  $240^\circ$  and  $280^\circ$   
211 show a relatively simple structure with one intra-crustal negative arrival as shown in Fig-  
212 ure 2. The dramatic change in receiver functions depending on the crust that is sampled,  
213 indicates the crustal structure below the different geological units is very different. There-  
214 fore it follows that the Bukit Timah fault is an approximately vertically dipping fault  
215 running throughout the crust. The presence of a significant fault also agrees with geo-  
216 logical information showing that the ages of the two units are very similar (Dodd et al.,  
217 2019; Oliver & Manka, 2014). This suggests that significant tectonic movement must have  
218 occurred in order for sedimentary rocks to be adjacent to a granite pluton that formed  
219 at the same time.

## 220 **6 Discussion and Conclusions**

221 We have generated robust receiver functions at high frequencies using a nodal ar-  
222 ray in a noisy urban environment. The method relies on 1) high receiver density allow-  
223 ing coherent signals to be identified and 2) man-made noise predominantly occurring at  
224 frequencies greater than 3 Hz. To create receiver function profiles across Singapore, we  
225 first de-noise the data by stacking. We stack both receiver functions from different earth-  
226 quakes and receiver functions from nearby stations. We also show for the first time that  
227 a temporary nodal array can be used for receiver function imaging using the popular com-  
228 mon conversion point method. The CCP method is a ray-based method and we suggest  
229 that future studies might profitably focus on wave-based migration methods (such as re-  
230 verse time migration (Chen et al., 2005)), which may prove superior with high receiver  
231 density (Shang et al., 2017). In this study, we do not invert for seismic velocity, since

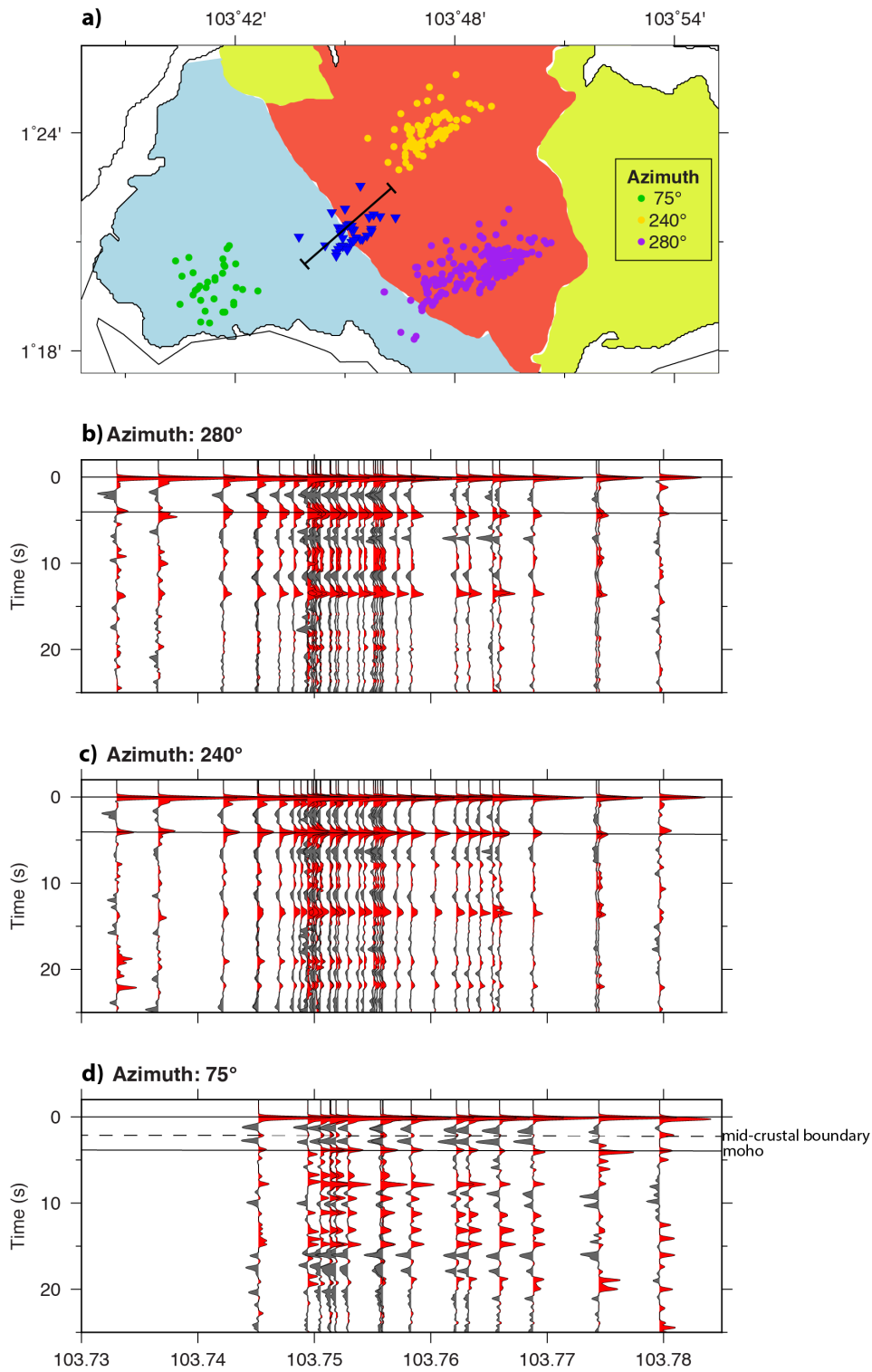


**Figure 4.** Azimuthal variations in receiver functions across Singapore. a) Map showing piercepoints where rays enter the base of the crust for three earthquakes from different azimuths. b) Receiver functions for seismic waves travelling at an azimuth of 280°. c) Receiver functions for seismic waves travelling at an azimuth of 240°. d) Receiver functions for seismic waves travelling at an azimuth of 75°.

232 receiver functions have low sensitivity to absolute seismic wave speed. Instead the re-  
233 ceiver functions presented here will be combined with surface waves in a joint inversion  
234 for 3D velocity structure.

235 Our results indicate a complex crustal structure beneath Singapore, reflecting Sin-  
236 gapore's complex geological history. In particular, azimuthal variations in receiver func-  
237 tions show distinct crustal structure below the Jurong Group and Bukit Timah gran-  
238 ite, confirming the presence of the Bukit Timah fault. Old faults in this area can be re-  
239 activated by distant stress fields from surrounding subduction zones. Therefore geolog-  
240 ical faults in and close-by to Singapore pose a seismic hazard to this densely populated  
241 area and warrant further characterisation.

## 242 **Acknowledgments**

243 We thank the Meteorological Service of Singapore for maintaining the 4 permanent seis-  
244 mic stations and for assistance with deploying nodes. We would also like to thank the  
245 following Singapore agencies for assistance in data acquisition: NParks, Ministry of Ed-  
246 ucation and the Public Utilities Board. We thank the Centre for Geohazard Observa-  
247 tion at NTU, along with all other field assistants for their help with the field survey, par-  
248 ticularly Jeffrey Encillo, Choong Yew Leong, Weiwen Chen and Mark Lim. Karen Lyth-  
249 goe is funded by an NTU Presidential Fellowship. We thank Kyle Bradley for useful dis-  
250 cussions on Singapore's geology and Wang Xin for assistance with receiver functions. Re-  
251 ceiver functions will be available for download from the Nanyang Technological Univer-  
252 sity data repository (*DOI to be provided*).

## 253 **References**

- 254 Chen, L., Wen, L., & Zheng, T. (2005). A wave equation migration method for re-  
255 ceiver function imaging: 1. theory. *J. Geophys. Res.*, *110*.
- 256 Dodd, T. J., Gillespie, M. R., Leslie, G. A., Kearsy, T. I., Kendall, R. S., Bide,  
257 T. P., ... Goay, M. (2019). Paleozoic to cenozoic sedimentary bedrock geology  
258 and lithostratigraphy of singapore. *J. of Asian Earth Sciences*, *180*.
- 259 ISC. (2019). International seismological centre on-line bulletin.  
260 doi: <https://doi.org/10.31905/D808B830>
- 261 Kosarev, G., Kind, R., Sobolev, S. V., Yuan, X., Hanka, W., & Oreshin, S. (1999).  
262 Seismic evidence for a detached indian lithospheric mantle beneath tibets.

- 263 *Proc. Natl. Acad. Sci. U.S.A.*, 283(5406), 1306–1309.
- 264 Langston, C. A. (1979). Structure under mount rainier, washington, inferred from  
265 teleseismic body waves. *J. Geophys. Res.*, 84, 4749–4762.
- 266 Leslie, G. A., Dodd, T. J., Gillespie, M. R., Kendall, R. S., Bide, T. P., Kearsey,  
267 M. R., Timothy I. and Dobbs, . . . Chiam, K. (2019). Ductile and brittle de-  
268 formation in singapore: A record of mesozoic orogeny and amalgamation in  
269 sundaland, and of post-orogenic faulting. *J. of Asian Earth Sciences.*, 180.
- 270 Ligorria, J. P., & Ammon, C. J. (1999). Iterative deconvolution and receiver-  
271 function estimation. *Bull. Seismol. Soc. Am.*, 89(5), 1395–1400.
- 272 Lin, F.-C. L., Li, D., Clayton, R. W., & Hollis, D. (2013). High-resolution 3d shal-  
273 low crustal structure in long beach, california: application of ambient noise  
274 tomography on a dense seismic array. *Geophysics*, 78(4), 45–56.
- 275 Liu, G., Persaud, P., & Clayton, R. W. (2018). Structure of the northern los angeles  
276 basins revealed in teleseismic receiver functions from short-term nodal seismic  
277 arrays. *Seism. Res. Lett.*, 89(5), 1680–1689.
- 278 Macpherson, K. A., Hidayat, D., Feng, L., & Goh, S.-H. (2013). Crustal thickness  
279 and velocity structure beneath singapore’s seismic network. *J. of Asian Earth  
280 Sciences.*, 64, 245–255.
- 281 Manning, T., Ablyazina, D., & Quigley, J. (2019). The nimble node — million-  
282 channel land recording systems have arrived. *The Leading Edge*, 706–714.
- 283 Oliver, Z. K. H. M. M. S., G. J. H., & Manka, T. (2014). U–pb zircon geochronol-  
284 ogy of early permian to late triassic rocks from singapore and johor: A plate  
285 tectonic reinterpretation. *Gondwana Research*, 26, 132–143.
- 286 Pan, T. C., & Sun, J. (1996). Historical earthquakes felt in singapore. *Bull. Seis-  
287 mol. Soc. Am.*, 86(4), 1173–1178.
- 288 Shang, X., V. de Hoop, M., & van der Hilst, R. D. (2017). Common conversion  
289 point stacking of receiver functions versus passive-source reverse time migra-  
290 tion and wavefield regularization. *Geophys. J. Int.*, 209(2), 923–934.
- 291 Shuib, M. K. (2009). The recent bukit tinggi earthquakes and their relationship to  
292 major geological structures. *Bull. of the Geological Soc. of Mal.*, 55, 67–72.
- 293 Sieh, K., Natawidjaja, D. H., Meltzner, A. J., Shen, C., Cheng, H., Li, K. S., . . .  
294 Edwards, R. L. (2008). Earthquake supercycles inferred from sea-level changes  
295 recorded in the corals of west sumatra. *Science*, 322, 1674–1678.

- 296 Vinnik, L. P. (1977). Detection of waves converted from p to sv in the mantle.  
297 *Phys. Earth Planet. Inter.*, 15(1), 39–45.
- 298 Wang, Y., Lin, F.-C., & Ward, K. M. (2019). Ambient noise tomography across the  
299 cascadia subduction zone using dense linear seismic arrays and double beam-  
300 forming. *Geophys. J. Int.*, 217, 1668–1680.
- 301 Ward, K. M., Lin, F., & Schmandt, B. (2018). High-resolution receiver function  
302 imaging across the cascadia subduction zone using a dense nodal array. *Geo-  
303 phys. Res. Lett.*, 24, 1054–1065.
- 304 Woon, L. K., & Yingxin, Z. (2009). *Geology of singapore* (2nd ed.). Defence Science  
305 and Technology Agency.
- 306 Zhu, L., Mitchell, B. J., Akyol, N., Cemen, I., & Kekovali, K. (2006). Crustal  
307 thickness variations in the aegean region and implications for the extension of  
308 continental crust. *J. Geophys. Res.*, 11.